

Optimisation of the receiver and recuperator of the small-scale open and direct solar thermal Brayton cycle for Pretoria

W.G. le Roux, T. Bello-Ochende and J.P. Meyer

Department of Mechanical and Aeronautical Engineering, University of Pretoria

Abstract

The net power output of the open and direct solar thermal Brayton cycle depends on the solar irradiation, wind, surrounding temperature and pressure of the location, as well as a few other geometric constants and parameters. These factors vary with time, day, and month. The geometries of the receiver and recuperator in the open and direct solar thermal Brayton cycle should be optimised in such a way that they accommodate the weather changes and allow for high net power output. In this paper, a method of obtaining these geometries based on total entropy generation minimisation is presented. The geometry of the receiver is obtained by optimising it for maximum solar irradiance. Once this optimum receiver geometry is found and kept constant, four recuperator geometries are identified which should be able to accommodate the different weather conditions (almost like the gears of a car which are used in different situations). In this work, a parabolic dish concentrator with a diameter of six meters is used as well as an off-the-shelf turbo-machine. The purpose of the paper is to show the advantage of changing the geometry of the recuperator in different weather conditions. Results show that the system with an optimised receiver and four recuperators performs well under certain weather conditions.

Keywords: receiver, recuperator, optimisation, solar, Brayton, entropy

Nomenclature

a	[m]	Longer side of rectangular recuperator channel
A	[m ²]	Area
b	[m]	Shorter side of rectangular recuperator channel
c_{p0}	[J/kgK]	Zero pressure constant pressure specific heat
CR	[-]	Concentration ratio
d	[m]	Receiver aperture diameter
dP	[-]	Pressure drop
D	[m]	Receiver diameter
D_{conc}	[m]	Concentrator diameter
D_{rec}	[m]	Receiver tube diameter
$D_{h,reg}$	[m]	Hydraulic diameter of recuperator channel
f	[-]	Friction factor
Gr	[-]	Grashof number
H	[m]	Recuperator height
I	[W/m ²]	Solar irradiance
k	[W/mK]	Thermal conductivity of a fluid
k	[-]	Gas constant (c_p / c_v)
L	[m]	Length
\dot{m}	[kg/s]	Mass flow rate
n	[-]	Number of flow channels
NTU	[-]	Number of transfer units
Nu	[-]	Nusselt number
P	[Pa]	Pressure
Pr	[-]	Prandtl number
\dot{Q}^*	[W]	Rate of intercepted heat at receiver cavity
\dot{Q}_{loss}	[W]	Rate of heat loss from the cavity receiver

\dot{Q}_{net}	[W]	Net rate of absorbed heat
r	[-]	Compressor pressure ratio
r_t	[-]	Turbine pressure ratio
R	[J/kgK]	Gas constant
Re	[-]	Reynolds number
R_f	[-]	Fouling factor
\dot{S}_{gen}	[W/K]	Entropy generation rate
t	[m]	Plate thickness between recuperator flow channels
T	[K]	Temperature
T^*	[K]	Apparent sun temperature as an exergy source
T_0	[K]	Environment temperature
V	[m/s]	Velocity
w	[-]	Wind factor
\dot{W}	[W]	Power
\dot{W}_{net}	[W]	Net power output of system
y	[-]	Numerical approximation constant
Z	[m]	Height
β	[-]	Inclination of receiver
ε	[-]	Effectiveness (in the ε - NTU method)
ρ	[kg/m ³]	Density
η	[-]	Efficiency
μ	[kg/ms]	Dynamic viscosity

Subscripts

0	Environment/loss
$1,2,3..$	Refer to Figure 1
c	Compressor
a	Receiver aperture
CF	Corrected flow
$conc$	Concentrator
D	Based on internal diameter of channel
h	Hydraulic
k	Channel
max	Maximum
min	Minimum
net	Net
rec	Receiver
reg	Recuperator
s	Surface
t	Turbine
th	Thermal
w	Receiver inner wall

1. Introduction

South Africa, like Southern Africa, has potential to generate large amounts of its power from solar technologies. The open Brayton cycle uses air as working fluid, which makes this cycle very attractive for use in the water-scarce Southern Africa. In the solar thermal Brayton cycle, rotational power can be generated using compressed and heated air. The turbine turns the compressor and the air is heated in the solar cavity receiver which absorbs the concentrated power of the sun. The system's exhaust consists of hot air which can be applied to heat water for domestic purposes, for space heating and/or to run

an absorption refrigerator. The small-scale open and direct solar thermal Brayton cycle with storage, could provide local energy for a small community.

The Brayton cycle is definitely worth studying when comparing its efficiency with those of other power cycles (Chen et al., 2007). To obtain the maximum net power output, a combined effort of heat transfer, fluid mechanics and thermodynamic thought is required. The method of entropy generation minimisation combines these thoughts (Bejan, 1982). The irreversibilities of the recuperative solar thermal Brayton cycle are mainly due to heat transfer across a finite temperature difference and fluid friction. For the solar thermal Brayton cycle with micro-turbine, Sendhil Kumar and Reddy (2008) suggests the use of a modified cavity receiver and Shah (2005) suggests the use of a counterflow plate-type recuperator. The geometries of these components should be optimised so that the system produces maximum net power output.

According to Bejan and Lorente (2010), on the topic of optimisation in nature, the best organ is not the infinitely large organ, as recommended by the thermodynamics of the organ alone. The best lung is imperfect since it destroys exergy by fluid friction. The imperfect component makes the whole animal or vehicle the least imperfect that it can be. It is with the same mind-set that the open and direct solar thermal Brayton cycle's components are optimised. In this work, however, it would be similar to giving a bird a choice between four lungs depending on the mode it is in and the mode which the environment is in. A lung which is optimised for flying, sitting and attacking can be used as examples. Just as a bird or variable geometry aircraft is able to change its wing's profile during different flight modes, the open and direct solar thermal Brayton cycle should be able to change the geometry of its recuperator to perform optimally in different environment conditions.

In recent work, a geometry optimisation method based on total entropy generation minimisation was developed and was applied to establish the maximum net power output of a small-scale open and direct solar thermal Brayton cycle with cavity receiver and recuperator at any steady-state condition (Le Roux et al., 2011a). This method allows for the global performance of the system to be optimised, by minimising the total irreversibility rate by sizing the receiver and recuperator accordingly, as suggested by various authors including Bejan et al. (1996). The net absorbed heat rate at the receiver was determined as a function of the receiver aperture diameter with the use of a receiver sizing algorithm by Stine and Harrigan (1985).

The effects of wind, receiver inclination, rim angle, atmospheric temperature and pressure, recuperator height, solar irradiance and concentration ratio on the optimum geometries and performance of the open and direct solar thermal Brayton cycle were also investigated by considering a single system in more detail (Le Roux et al., 2011b). The solar irradiance, wind, inclination and temperature, change throughout the day, and also throughout the year. In recent work it was found that the solar inclination and radiation are the most important and significant changes which occur throughout the day (Le Roux et al., 2011c). The change in solar irradiance changes the maximum net power output of the system as well as the optimum geometries (of receiver and recuperator) and optimum operating point of the micro-turbine. A change in temperature, pressure, inclination and wind, however, does not change the optimum operating point, but just changes the optimum geometries.

The open and direct solar thermal Brayton cycle should thus be optimised to operate over a period of time, since the environment in which it is situated and its heat source are functions of time. This can be done by taking into consideration the probability of certain environmental conditions being present throughout the year. Approximations for solar irradiance based on time and location are available. Bakirci (2008) developed a

correlation equation giving monthly averages of clear-sky and global solar radiation on horizontal surfaces in Erzurum, Turkey. According to Wong and Chow (2001), the best database would be the long-term measured data at the site of the proposed solar system, however, the limited coverage of radiation measuring networks dictates the need for developing solar radiation models. Wong and Chow (2001) reviewed a number of solar radiation models. For the selected weather conditions in this paper, the net power output of the system is maximised, the total entropy generation rate is minimised and the geometries of the receiver and recuperator are optimised.

2. Proposed model

The open and direct solar thermal Brayton cycle with recuperator is shown in Fig. 1. A six metre diameter parabolic concentrator concentrates the solar heat for the cavity receiver. The specular reflectivity of the concentrator is assumed to be 85%. The rate of intercepted heat by the cavity receiver, \dot{Q}^* , depends on the cavity receiver aperture (which depends on the geometries of the cavity receiver). \dot{W}_{net} is the net power output of the system.

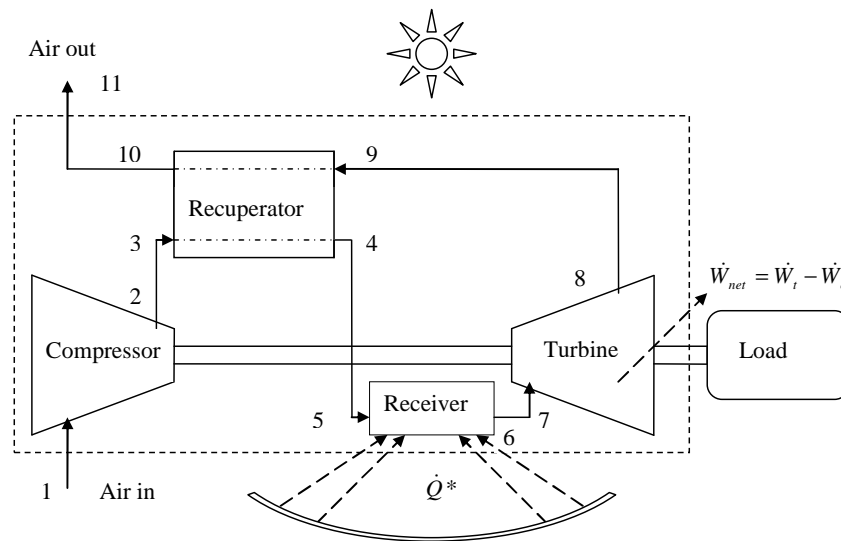


Figure 1. The open and direct solar thermal Brayton cycle with recuperator.

2.1. Solar receiver model

The modified cavity receiver suggested by Reddy and Sendhil Kumar (2009) is shown in Fig. 2. The receiver inner surface is made up of closely wound copper tubing with diameter, D_{rec} , through which the working fluid travels. The receiver tube with length, L_{rec} , constructs the cavity receiver and its aperture. The convection heat loss takes place through the receiver aperture with diameter, d . An area ratio of $A_w / A_a = 8$ is recommended by Reddy and Sendhil Kumar (2009) as it was found to be the ratio that gives the minimum heat loss from the cavity receiver. Since the surface area of a sphere is πD^2 , the diameter of the spherical receiver can be calculated as

$$D = 2\sqrt{(A_w + A_a)/3\pi} \quad (1)$$

Due to the area ratio constraint, the receiver diameter is a function of the receiver aperture diameter,

$$D = \sqrt{3d} \quad (2)$$

The receiver aperture diameter can be calculated using equation (3) since $A_w = D_{rec}L_{rec}$.

$$d = \sqrt{D_{rec} L_{rec} / 2\pi} \quad (3)$$

According to Reddy and Sendhil Kumar (2008), the total rate of heat loss due to convection and radiation, can be approximated (Le Roux et al., 2011a) as

$$\dot{Q}_{loss} \approx 1.396 Gr_D^{0.209} (1 + \cos \beta)^{0.968} (T_w / T_0)^{-0.317} (d / D)^{0.425} (k A_a / D) (T_w - T_0) \quad (4)$$

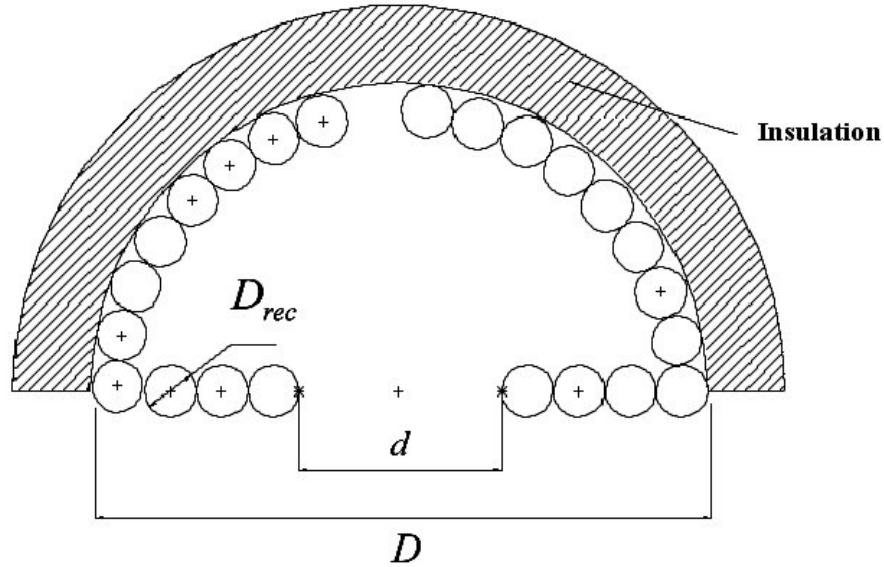


Figure 2. Modified cavity receiver.

2.2. Determination of net absorbed power

In practise, at the focal point of a solar concentrator, the reflected rays do not form a point but form an image of finite size centred about the focal point. This is due to the sun's rays not being truly parallel and due to concentrator errors. For the concentrator with constant diameter, focal length and rim angle, the net rate of heat absorbed by the working fluid in the receiver depends on the receiver aperture diameter. The larger the receiver aperture diameter, the larger the rate of heat intercepted by the receiver, \dot{Q}^* . Also, the larger the aperture diameter, the larger the heat loss rate, \dot{Q}_{loss} , due to convection and radiation in equation (4). The net rate of absorbed heat, \dot{Q}_{net} , is the intercepted heat rate minus the total heat loss rate. The sizing algorithm of Stine and Harrigan (1985) is applied to determine \dot{Q}^* for a specific aperture diameter. The sizing algorithm uses the concentrator area, rim angle, specular reflectance, inclination, irradiance, parabolic concentrator error and heat loss rate to determine the net absorbed heat rate as a function of the receiver aperture diameter. The shadow of the receiver and its insulation is also accounted for when calculating the intercepted heat rate.

$$\dot{Q}_{net} = \sum_{i=0}^{10} y_i d^i \quad (5)$$

The net absorbed heat rate as a function of receiver aperture diameter, from the sizing algorithm, can be numerically approximated with equation (5) using the discrete least squares approximation method (Burden and Faires, 2005), where y_i is a set of constants used to describe the function.

2.3. Recuperator model

A counterflow plate-type recuperator is used as shown in Fig. 3. The channels with hydraulic diameter, $D_{h,reg}$, length, L_{reg} , and aspect ratio, a/b_{reg} are shown. The number of

flow channels in the recuperator, n , depends on the recuperator height, H , channel height, b , and thickness of the channel separating surface, t , and can be written as a function of the channel aspect ratio,

$$n = H / (t + b) = \frac{H}{t + D_{h,reg} \left(\left(\frac{a}{b} \right)_{reg} + 1 \right) / \left(2 \left(\frac{a}{b} \right)_{reg} \right)} \quad (6)$$

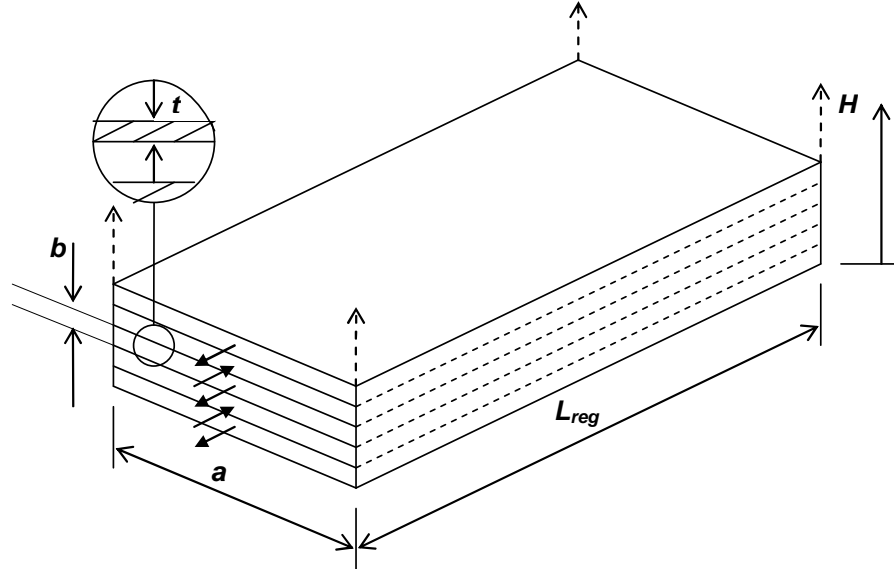


Figure 3. Counterflow plate-type recuperator.

Equation (7) gives the mass flow rate per channel.

$$\dot{m}_k = 2\dot{m} / n \quad (7)$$

The surface area, A_s , for a channel as a function of the channel aspect ratio is

$$A_s = 2(a + b)L_{reg} = D_{h,reg} L_{reg} \left(\left(\frac{a}{b} \right)_{reg} + 1 \right) \left(1 + \left(\frac{a}{b} \right)_{reg}^{-1} \right) \quad (8)$$

The thickness of the material between the hot and cold stream, t , is 1 mm and the recuperator height is 1 m. The Reynolds number for a flow channel is

$$Re = \dot{m}_k D_{h,reg} \left(\frac{a}{b} \right)_{reg} / \mu a^2 \quad (9)$$

Using the definition of the hydraulic diameter and equation (9), the Reynolds number can be calculated with

$$Re = \frac{4 \left(\frac{a}{b} \right)_{reg} \dot{m}_k}{\mu D_{h,reg} \left(\left(\frac{a}{b} \right)_{reg} + 1 \right)^2} \quad (10)$$

Heat exchanger irreversibilities can be reduced by slowing down the movement of fluid through a heat exchanger (Bejan, 1982). Small Reynolds numbers can thus be expected for the optimised recuperator channels and the Gnielinski equation (Gnielinski, 1976) can be used to determine the Nusselt number,

$$Nu_D = (\text{Pr}(\text{Re}-1000)(f/8)) / \left(1 + 12.7(f/8)^{0.5} \left(\text{Pr}^{2/3} - 1\right)\right) \quad (11)$$

The Petukhov equation (Petukhov, 1970) is used to calculate the friction factor,

$$f = (0.79 \ln \text{Re} - 1.64)^{-2} \quad (12)$$

With the use of the friction factor, Reynolds number and the definition of the pressure drop (Çengel, 2006), the pressure drop through the recuperator can be written in terms of the geometric variables as

$$\Delta P = \left(0.79 \ln \frac{4\dot{m}_k (a/b)_{reg}}{\mu D_{h,reg} (a/b_{reg} + 1)^2} - 1.64\right)^{-2} \left(\frac{8\dot{m}_k^2 (a/b)_{reg}^2}{\rho (a/b_{reg} + 1)^4}\right) \left(L_{reg} / D_{h,reg}^5\right) \quad (13)$$

2.4. Compressor and turbine properties

A standard off-the-shelf micro-turbine is used in the analysis (Garrett, 2009). The compressor pressure ratio ($r = P_2/P_1$) can be chosen to be a parameter when considering geometric optimisation (Snyman, 2009). The compressor efficiency, mass flow rate, compressor pressure ratio and turbine pressure ratio are intrinsically coupled to each other.

3. Research methodology

3.1. Variables

There are five geometric variables to be optimised: The cavity receiver tube diameter, D_{rec} , the tube length of the cavity receiver, L_{rec} , the hydraulic diameter of the recuperator channels, $D_{h,reg}$, the length of the recuperator channels, L_{reg} , and aspect ratio of the recuperator channels, a/b_{reg} . The objective function (net power output of the system) in terms of the scaled geometry variables, parameters and constants is maximised using the dynamic trajectory optimisation method by Snyman (2000) in MATLAB.

3.2. Selection of most common weather conditions

Table 1. The proposed four most common weather conditions for Pretoria.

Weather condition	Inclination, β	Solar Irradiation, I (W/m ²)	Wind factor, w	Temperature (°C)
A	15°	285	2.5	15
B	25°	465	2.3	18
C	41°	722	1.5	21
D	87°(90°)	1098 (1200)	2.5 (1)	30 (40)

The hourly solar inclination for Pretoria was determined for each day of the year between 07:00 and 17:00 using SunEarthTools (2001). After speculation and considering the maximum solar radiation during summer and winter, it was assumed that the clear-sky solar radiation is a function of the inclination of the collector as shown in equation (14):

$$I = \sin(\beta) \times 1100 \quad (14)$$

The average monthly wind conditions and temperatures were also obtained. Using a weighting factor and probability of occurrence, four most common weather conditions were identified and are shown in Table 1. To prevent tube burnout, condition D was altered (values in brackets) to present a situation where the heat transfer into the receiver would be the maximum.

3.3. Modelling and the objective function

The objective function is the function which is maximised by the optimisation of variables. The net power output of the system should be written in terms of the total entropy generation rate in the system. The entropy generation mechanisms are identified and the objective function is constructed. For each weather condition, the optimisation of the geometry variables is done over a range of operating points of the micro-turbine. For weather condition D, the optimised geometry of the receiver at the operating point which allows for highest maximum net power output, is used as fixed receiver geometry for the optimisation of the recuperators at the other three weather conditions.

3.3.1. Temperatures and pressures in terms of geometry variables

The modelling of the temperatures and pressures is required since the objective function requires the values of the temperatures and pressures at each point in Fig. 1. It is assumed that $P_1 = P_{10} = P_{11} = 86$ kPa (see Fig. 1). The temperatures and pressures in all the ducts are calculated with an assumed temperature loss or pressure drop which is small.

Any turbo-machine has a compressor and turbine map. Zhuge et al. (2009) shows experimental results for turbines and their mass flow rates. It is assumed that the turbine corrected mass flow rate and turbine pressure ratio can be modelled with the use of the turbine map. The turbine map shows at which corrected mass flow rates and pressure ratios the turbine is able to operate. For each chosen weather condition, each of these operating points is considered. Three iterations are required. After choosing the turbine operating point, T_7 is chosen for the first iteration. For the second iteration, the system mass flow rate is guessed, where after dP_{9-10} , P_9 , P_8 and P_7 are calculated so that the mass flow rate can be calculated using equation (15),

$$\dot{m}_t = \frac{\dot{m}_{cCF} \times P_7 / 14.7}{\sqrt{(T_7 + 460) / 519}} \quad (15)$$

where P_7 is in psi and T_7 in degrees Fahrenheit respectively (Garrett, 2009).

The corrected compressor mass flow rate can then be calculated with equation (16) since the mass flow rate through the compressor is equal to the mass flow rate through the turbine.

$$\dot{m}_{cCF} = \frac{\dot{m} \times \sqrt{(T_1 + 460) / 545}}{P_1 / 13.95} \quad (16)$$

Note that P_1 and T_1 are in psi and degrees Fahrenheit respectively (Garrett, 2009). For the third iteration, the compressor pressure ratio is guessed so that dP_{3-4} , P_6 , P_5 , P_4 , P_3 and P_2 can be calculated. This allows for the compressor pressure ratio to be obtained with iteration.

The compressor isentropic efficiency can be read from the compressor map using the corrected compressor mass flow rate and compressor pressure ratio. A turbine isentropic efficiency of 0.8 is assumed since it is a function of the load (Tveit et al., 2005). Thus the more power the micro-turbine is able to produce the larger the allowable load and the higher the efficiency. The recuperator efficiency is calculated using the ε - NTU method with the fouling factor for air given as $R_f = 0.004$ (Çengel, 2006), where after the temperatures can be found so that T_7 can be iterated.

3.3.2. Construction of the objective function

The finite heat transfers and pressure drops in the compressor, turbine, recuperator, receiver and ducts are identified as entropy generation mechanisms. When doing an exergy analysis for the system and assuming $V_1 = V_{11}$ and $Z_1 = Z_{11}$, the objective function can be assembled as given in equation (17). The function to be maximised (the objective function), is \dot{W}_{net} (the net power output). Equation (18) shows the total entropy generation rate in terms of the temperatures and pressures (with reference to Fig. 1). The entropy generation rate for each component is added and is shown in block brackets. For the analysis in this work, T^* is assumed to be 2 470 K (Bejan, 1982) and at a point between the concentrator and receiver.

$$\dot{W}_{net} = -T_0 \dot{S}_{gen} + \left(1 - \frac{T_0}{T^*}\right) \dot{Q}^* + \dot{m} c_{p0} (T_1 - T_{11}) - \dot{m} T_0 c_{p0} \ln(T_1 / T_{11}) \quad (17)$$

where

$$\begin{aligned} \dot{S}_{gen} = & \left[-\dot{m} c_{p0} \ln(T_1 / T_2) + \dot{m} R \ln(P_1 / P_2) \right]_{compressor} \\ & + \left[\dot{Q}_0 / T_0 + \dot{m} c_{p0} \ln(T_3 / T_2) - \dot{m} R \ln(P_3 / P_2) \right]_{Duct\ 23} \\ & + \left[\dot{m} c_{p0} \ln \left[\frac{T_{10} T_4}{T_9 T_3} \left(\frac{P_{10} P_4}{P_9 P_3} \right)^{(1-k)/k} \right] + \dot{Q}_0 / T_0 \right]_{recuperator} \\ & + \left[\dot{Q}_0 / T_0 + \dot{m} c_{p0} \ln(T_5 / T_4) - \dot{m} R \ln(P_5 / P_4) \right]_{Duct\ 45} \\ & + \left[-\frac{\dot{Q}^*}{T^*} + \frac{\dot{Q}_{loss}}{T_0} + \dot{m} c_{p0} \ln(T_6 / T_5) - \dot{m} R \ln(P_6 / P_5) \right]_{receiver} \\ & + \left[\dot{Q}_0 / T_0 + \dot{m} c_{p0} \ln(T_7 / T_6) - \dot{m} R \ln(P_7 / P_6) \right]_{Duct\ 67} \\ & + \left[-\dot{m} c_{p0} \ln(T_7 / T_8) + \dot{m} R \ln(P_7 / P_8) \right]_{turbine} \\ & + \left[\dot{Q}_0 / T_0 + \dot{m} c_{p0} \ln(T_9 / T_8) - \dot{m} R \ln(P_9 / P_8) \right]_{Duct\ 89} \end{aligned} \quad (18)$$

Note that $\dot{Q}^* - \dot{Q}_{loss} = \dot{Q}_{net}$.

3.3.3. Constraints

The recuperator aspect ratio is constrained to a maximum of 250. The concentration ratio between concentrator area and receiver aperture area, CR is constrained to $CR_{min} = 100$.

$$D_{h,rec} L_{rec} / 8 - A_{s,conc} / CR_{min} \leq 0 \quad (19)$$

Equation (20) prevents the receiver from losing its cavity shape, by only allowing a minimum of two diameters in the distance between the aperture edge and the edge of the receiver.

$$2D_{h,rec} - \left((\sqrt{3} - 1) / 2 \right) \sqrt{D_{h,rec} L_{rec} / 2\pi} \leq 0 \quad (20)$$

The cavity receiver tubes are constructed from copper. The maximum surface temperature of the receiver tubes should stay well below its melting temperature. A maximum receiver surface temperature of $T_{s,max}$ is identified for the analysis (Shah, 2005 and Garrett, 2009). The surface area of a tube and the Dittus-Boelter equation (Dittus and Boelter, 1930) help to construct equation (21), which is the maximum surface temperature of the receiver.

$$T_{s,max} = T_6 + \dot{Q}_{net} / \left(0.023\pi L_{rec} k Pr^{0.4} \left(4\dot{m} / (\mu\pi D_{h,rec}) \right)^{0.8} \right) \quad (21)$$

The longer the recuperator the more beneficial it is to the system. There needs to be a constraint on its length. To make sure the system stays compact, the recuperator's length cannot exceed the length of the radius of the dish,

$$L_{reg} \leq D_{conc} / 2 \quad (22)$$

4. Results

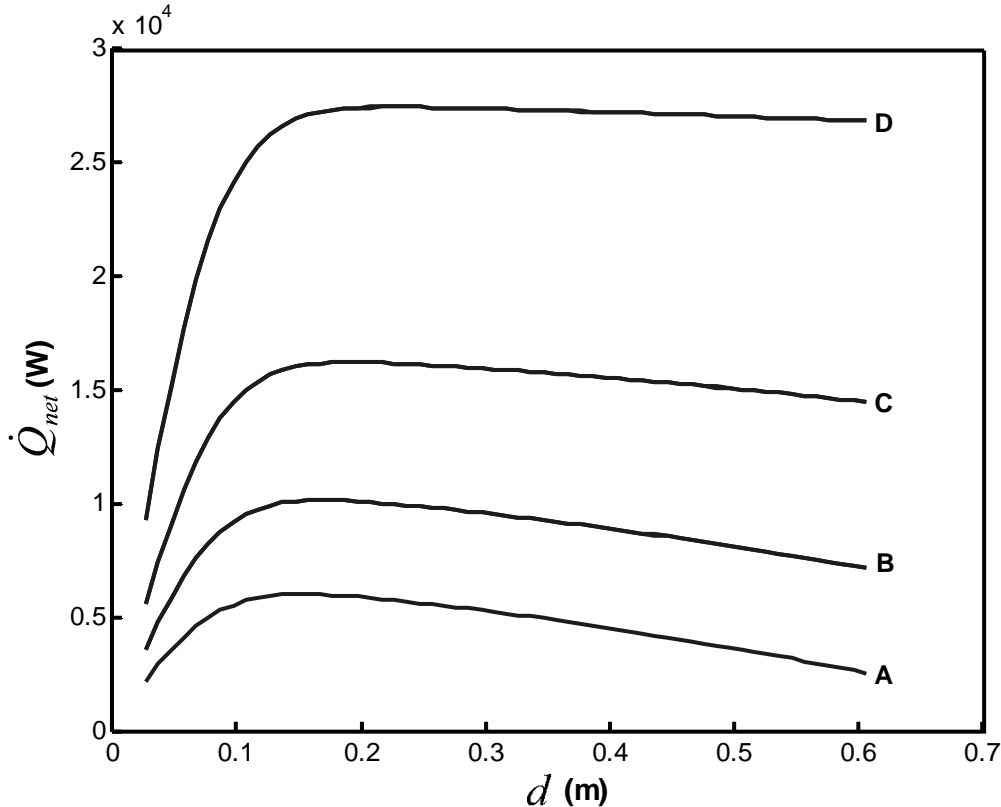


Figure 4. Net absorbed heat rate at cavity receiver depending on cavity receiver aperture diameter.

Figure 4 shows the relation between \dot{Q}_{net} and the receiver aperture diameter for each of the proposed most common weather conditions in Table 1. Note that Fig. 4 was generated

by using a parabolic concentrator error of 0.0067 rad and rim angle of 45° as suggested by Stine and Harrigan (1985).

For each of the proposed weather conditions in Table 1, the objective function was maximised at different operating points of the turbo-machine's turbine, as shown on its turbine map. These results are shown in Fig. 5 as a function of compressor pressure ratio. Note that there exists an operating point for each weather condition, which provides the highest maximum net power output. The operating points with the highest maximum net power outputs and their optimum geometries for each weather condition are shown in Table 2. These operating points are also shown in Fig. 6 where the compressor map is shown. Note that for weather conditions A, B and C, the geometry of the receiver was fixed at the optimum geometry found for weather condition D.

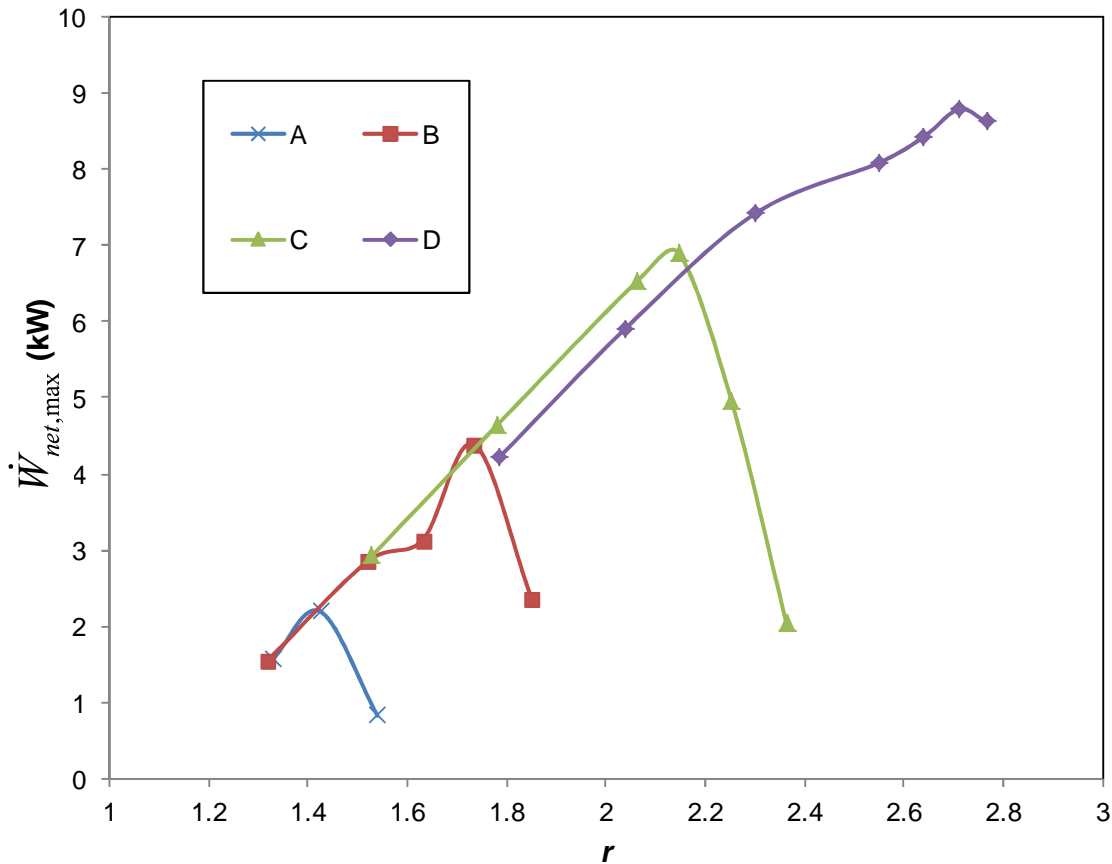


Figure 5. Maximum net power output at different operating points of the micro-turbine at the four different weather conditions.

Table 2. Operating points with highest maximum net power output for each of the four weather conditions.

	r	$\dot{m}_{t,CF}$ (kg/s)	r_t	$\dot{m}_{t,CF}$ (lb/min)	\dot{m} (kg/s)	T_7 (K)	D_{rec} (cm)	L_{rec} (m)	a/b_{re} g	$D_{h,re}$ g (mm)	L_{re} g (m)	W_{net} (W)
D*	2.7 2	0.11	2.6 5	11.2	0.1	112 9	6.81	18. 1	31.51	6.69 6	3	8788
C*	2.1 5	0.08	2.1	11	0.08	110 3	6.81	18. 1	250	5.63 4	3	6901
B*	1.7 3	0.06	1.7	10	0.06	115 4	6.81	18. 1	250	6.61 8	3	4393
A*	1.4 3	0.04	1.4	8.5	0.04	117 5	6.81	18. 1	150	6.64	1.1	2194

To establish whether these four recuperators and the receiver are able to handle the various weather conditions throughout a typical year, a few other weather conditions are considered. Note that each of these recuperators is optimised for the weather conditions listed in Table 2. A recuperator should be able to handle solar radiation cases which are below and close to the value for which it was optimised, so that tube burnout does not occur. It is also important that the micro-turbine should be able to operate within its compressor map range (Fig. 6) at the different weather conditions, otherwise flow surge or choking can occur. Table 3 shows the results. For test number 1 to 6, recuperator D was used. Note how the system performs well as the weather condition is close to the weather condition this recuperator was optimised for (shown in Table 1). The decrease in solar radiation has a large effect on the net power output of the system. When the solar radiation falls below $1\,000\text{ W/m}^2$, the system is unable to generate a positive net power output. The effect of wind and temperature is also shown. These factors do not decrease the net power output tremendously. The operating points on the compressor map are also listed in Table 3. Note that test number 5 goes off the compressor map. The system performs well between $1\,000$ to $1\,200\text{ W/m}^2$ ($\eta_{th} \leq 26\%$) when using recuperator D.

1	1100	1	90	305	2.72	0.118	1023	5840
2	1100	1	90	300	2.72	0.117	1019	6054
3	1000	1	65.4	300	2.73	0.129	842	2295
4	900	1	54.9	300	2.74	0.14	699	-1362
5	800	1	46.7	300	2.75	0.155	579	-5056
6	1100	2	90	300	2.72	0.12	982	5326
C								
7	700	1	39.5	295	2.15	0.084	1150	6756
8	600	1	33.1	295	2.155	0.099	823	3133
9	500	1	27	295	2.17	0.124	532	-1714
10	800	1	46.7	300	2.14	0.072	1556	9872
B								
11	400	1	21.3	291	1.74	0.061	1134	4116
12	300	1	15.8	291	1.75	0.089	544	184
13	300	2	15.8	291	1.77	0.11	356	-2457
14	500	1	27	295	1.73	0.048	1887	7095
A								
15	200	1	10.5	288	1.43	0.047	919	1497
16	200	2	10.5	288	1.44	0.068	440	-211
17	300	2	15.8	291	1.42	0.033	1861	3286
18	300	1	15.8	291	1.42	0.028	2726	4548

5. Conclusions and recommendations

The optimised receiver and recuperators of the open and direct solar thermal Brayton cycle performs well in certain weather conditions. The results show that tube burnout is a problem when optimising the receiver and recuperator geometries to operate in a constantly changing environment. Results showed that when a recuperator is optimised for a specific weather condition, it allows the system to also perform well at other weather conditions which are close to the condition it was optimised for. This is true when the solar radiation is lower than the radiation the recuperator was optimised for. When the radiation is higher, it causes tube burnout. Tube burnout might be prevented by introducing concentrator shading, rejection of solar radiation or flow bypass. One could also consider adding extra recuperators at the troubled regions or consider investigating the possibility of placing the existing recuperators in series or parallel, so that the system would be able to perform in all the weather conditions. Future work could also include the addition of cost constraints and looking at other micro-turbines for better results.

References

- Bakirci, K., 2008. Correlations for Estimation of Solar Radiation on Horizontal Surfaces. *Journal of Energy Engineering*. 134 (4). ISSN 0733-9402/2008/4-130–134/\$25.00.
- Bejan, A., *Entropy Generation through Heat and Fluid Flow*, John Wiley & Sons, Inc., Colorado, 1982.
- Bejan, A., Tsatsaronis, G. and Moran, M., *Thermal design and optimization*, John Wiley & Sons, Inc., New York, 1996.
- Bejan, A., and Lorente, S., 2010. The constructal law of design and evolution in nature.

Philosophical Transactions of the Royal Society Biological Sciences. 365, p. 1335-1347. doi: 10.1098/rstb.2009.0302.

Burden, R. L. and Faires, J. D., *Numerical Analysis*, 8th ed, Thomson Brooks/Cole, Youngston State University, 2005.

Çengel, Y. A., *Heat and Mass Transfer*, 3rd ed, McGraw-Hill, Nevada, Reno, 2006.

Dittus, F. W. and Boelter, L. M. K., University of California publications on engineering, Vol.2, 1930, pp. 433.

Chen L., Zhang, W. and Sun, F., Power, efficiency, entropy-generation rate and ecological optimization for a class of generalized irreversible universal heat-engine cycles, *Applied Energy*, Vol. 84, 2007, pp. 512-525.

Dittus, F. W. and Boelter, L. M. K., University of California publications on engineering, Vol.2, 1930, pp. 433.

Garrett, Garrett by Honeywell: turbochargers, intercoolers, upgrades, wastegates, blow-off valves, turbo-tutorials, 2009, Available at: <http://www.TurboByGarrett.com> [Accessed 26 April 2010].

Gnielinski, V., New equations for heat and mass transfer in turbulent pipe and channel flow, *International Chemical Engineering*, Vol. 16, 1976, pp. 359-368.

Le Roux WG, Bello-Ochende T, Meyer JP. Thermodynamic optimisation of an integrated design of a small-scale solar thermal Brayton cycle. *International Journal of Energy Research*; 2011a. doi:10.1002/er.1859.

Le Roux WG, Bello-Ochende T, Meyer JP. Operating conditions of an open and direct solar thermal Brayton cycle with optimised cavity receiver and recuperator. *Energy*; 2011b. doi:10.1016/j.energy.2011.08.012.

Le Roux, W.G., Bello-Ochende, T. and Meyer, J.P., 2011c. Optimum performance of the small-scale open and direct solar thermal Brayton cycle at various environmental conditions and constraints. *Energy*. Manuscript number: EGY-D-11-01454. Accepted for review on 2011/09/03.

Petukhov, B. S., Heat transfer and friction in turbulent pipe flow with variable physical properties, *Advances in Heat Transfer*, Vol. 6, 1970.

Reddy, K. S. and Sendhil Kumar, N., Combined laminar natural convection and surface radiation heat transfer in a modified cavity receiver of solar parabolic dish, *International Journal of Thermal Sciences*, Vol. 47, 2008, pp. 647–1657.

Reddy, K. S. and Sendhil Kumar, N., An improved model for natural convection heat loss from modified cavity receiver of solar dish concentrator, *Solar Energy*, Vol. 83, 2009, pp. 1884–1892.

Sendhil Kumar, N. and Reddy, K. S., Comparison of receivers for solar dish collector system, *Energy Conversion and Management*, Vol. 49, 2008, pp. 812-819.

Shah, R. K., Micro Gas Turbines, 2, *Compact Heat Exchangers for Microturbines*, Neuilly-sur-Seine, France: RTO, 2005, pp. 2-1 – 2-18. Available from: <http://www.rto.nato.int/abstracts.asp>.

Snyman, J.A., The LFOPC leap-frog algorithm for constrained optimization, *Computers and Mathematics with Applications*, Vol. 40, 2000, pp. 1085-1096.

Snyman, J. A., *Practical Mathematical Optimization*, University of Pretoria, Pretoria, 2009.

Stine, B.S. and Harrigan, R.W., *Solar Energy Fundamentals and Design*, John Wiley & Sons, Inc., New York, 1985.

SunEarthTools. 2011. *SunEarthTools.com, Tools for consumers and designers of solar*. Available at: http://www.sunearthtools.com/dp/tools/pos_sun [2011/10/20]

Tveit, T.M., Savola, T. and Fogelholm, C.J. Modelling of steam turbines for mixed integer nonlinear programming (MINLP) in design and off-design conditions of CHP plants. In: SIMS 2005, 46th Conference on Simulation Modeling, 2005, pp. 335–344.

Wong, L.T., Chow, W.K., 2001. Solar radiation model. *Applied Energy*. 69 , p. 91–224.

Zhuge, W., Zhang, Y., Zheng, X, Yang, M. and He, Y., 2009. Development of an advanced turbocharger simulation method for cycle simulation of turbocharged internal combustion engines. *Proceedings of the Institution of Mechanical Engineers, Part D: Journal of Automobile Engineering*. 223: 661. DOI: 10.1243/09544070JAUTO975.